IOP Publishing Superconductor Science and Technology
Supercond. Sci. Technol. 31 (2018) 075007 (8pp) https://doi.org/10.1088/1361-6668/aac614

Numerical simulation of magnetic field for compact electromagnet consisting of REBCO coils and iron yoke

Shuangrong You, Changxin Chi, Yanqun Guo, Chuanyi Bai, Zhiyong Liu, Yuming Lu and Chuanbing Cai[1]

Shanghai Key Laboratory of High Temperature Superconductors, Physics Department, College of Sciences, Shanghai University, Shanghai 200444, People's Republic of China

E-mail: cbcai@shu.edu.cn

Received 22 January 2018, revised 29 April 2018
Accepted for publication 18 May 2018
Published 8 June 2018

Abstract

This paper presents the numerical simulation of a high-temperature superconductor electromagnet consisting of REBCO (RE-$Ba_2Cu_3O_{7-x}$, RE: rare earth) superconducting tapes and a ferromagnetic iron yoke. The REBCO coils with multi-width design are operating at 77 K, with the iron yoke at room temperature, providing a magnetic space with a 32 mm gap between two poles. The finite element method is applied to compute the 3D model of the studied magnet. Simulated results show that the magnet generates a 1.5 T magnetic field at an operating current of 38.7 A, and the spatial inhomogeneity of the field is 0.8% in a Φ–20 mm diameter sphere volume. Compared with the conventional iron electromagnet, the present compact design is more suitable for practical application.

Keywords: HTS electromagnet, REBCO, 3D simulation, finite element method, iron yoke, 77 K, multi-width

(Some figures may appear in colour only in the online journal)

1. Introduction

REBCO-coated conductors with a Hastelloy or stainless-steel substrate exhibit large in-field current carrying capacity and outstanding axial mechanical performance [1]. For magnetic wire, the above-mentioned properties ensure the reliability of the magnet in high field with huge Lorentz force. The REBCO tape-based magnets are investigated concentrating mostly on high field at low temperature [1, 2]. For instance, the National High Magnetic Field Laboratory (NHMFL) reported a 35.4 T field generated by a 4.2 T REBCO insert coil placed in a 31.2 T background magnet [3]. In addition, a 26 T all-REBCO magnet designed by the MIT Francis Bitter Magnet Laboratory, was constructed by the SuNAM Co., Ltd [4]. More recently, the NHMFL presented a 32 T all-superconducting magnet made with two REBCO insert coils and a low-temperature superconductor (LTS) background magnet [5, 6]. Few of the studies are aimed at the potential applications for REBCO tapes in relatively low field, for which wide demand for general use exists, as with conventional iron electromagnets.

REBCO-coated conductors exhibit a critical temperature (T_c) as high as 92 K, which allows the necessary working environment in liquid nitrogen (LN_2), a kind of cheap and easy cryogenics for large-scale applications. The in-field current carrying capacity of REBCO tape, however, is much lower at 77 K than that at low temperature. It is hard to achieve a magnetic field of more than 1 T, in spite of the high consumption of REBCO tapes. Combining them with a ferromagnetic iron yoke/core to concentrate the magnetic flux is a way to apply high-temperature superconductor (HTS) tapes at relatively high temperature, e.g. the synchrotron dipole magnets [7]. Nevertheless, most of them are built by bismuth strontium calcium copper oxide tape at present and virtually none of them are designed to work at 77 K without refrigeration. In the present work, a 77 K HTS electromagnet consisting of REBCO coils and an iron yoke (hereinafter referred to as a 'REBCO iron electromagnet'), with compact design and lower consumption of REBCO tapes, is investigated.

[1] Author to whom any correspondence should be addressed.

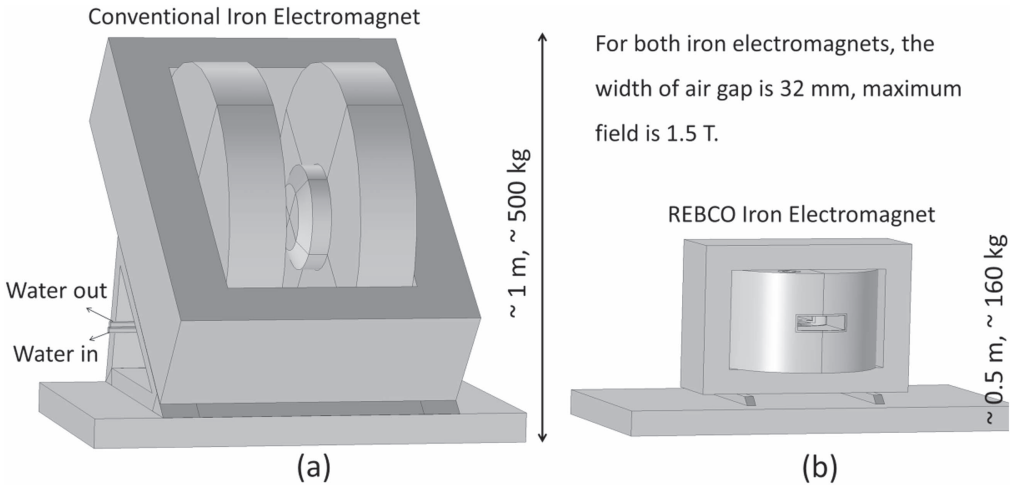

Figure 1. Conventional iron electromagnet is widely applied to provide a 0–2 T magnetic field. It is commercial, but cumbersome. Present design is expected to reduce whole magnet size with lower power consumption. (a) Sketch of H-Frame conventional iron electromagnet, (b) sketch of REBCO iron electromagnet.

The advantages of the present design include, no refrigeration, reduced cost compared to a normal LTS magnet, and compact size, allowing better adaption compared with a conventional iron electromagnet (figure 1). This design is expected to be applicable in many situations where conventional iron electromanets are used such as an external magnetic source for instruments, sample magnetization, magnetic annealing, electron paramagnetic resonance, magneto-optical, etc. Recently, we investigated an external magnetic source for differential scanning calorimeter application, which needs a 1.5 T maximum field, spatial inhomogeneity better than 1% within a 20 mm (distance between testing sample and standard sample in the calorimeter head) diameter sphere volume (DSV), and at least a 30 mm room-temperature gap. The following work is proposed according to this practical demand.

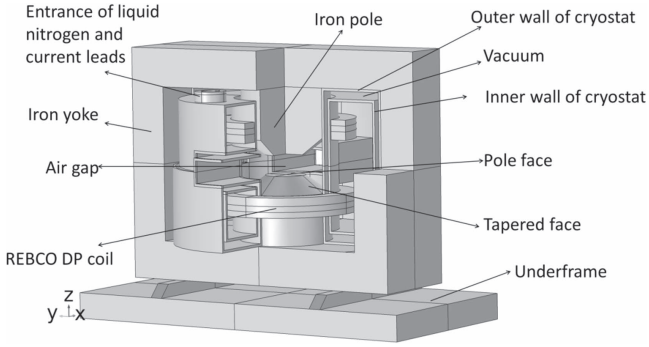

Figure 2. Structure of the REBCO iron electromagnet. An iron pole is surrounded by the REBCO coil. Special LN_2 cryostat is designed to ensure the iron pole works at room temperature while the REBCO coil operates at 77 K. The iron yoke is an H-Frame, but is rotated 90°.

2. Design and 3D model of the REBCO iron electromagnet

2.1. Design of the structure

Generally, the REBCO iron electromagnet is designed following the structure of a conventional iron electromagnet, where copper coils and a water cooling system are replaced by REBCO coils and a liquid nitrogen (LN_2) cryostat, respectively. Figure 2 demonstrates the whole structure of the REBCO iron electromagnet. It mainly consists of three parts, including two REBCO coils, an electrical pure iron yoke and poles, and a LN_2 cryostat.

Each REBCO coil is assembled by three REBCO double pancakes (DPs). The radial component of magnetic field (B_r) in the DPs is a key parameter in this case, as it will decrease the operating current significantly as it is perpendicular to the winding tape (or parallel to the *c*-axis of the REBCO tape). By the multi-width winding technique [8, 9], the wider-tape DPs are placed at the sections where the B_r limits the REBCO tape performance. To enhance the center field in the gap with lower B_r in the coils, the distance between the two REBCO coils is adjusted to 70 mm. The ferromagnetic iron yoke and poles serve as a magnetic flux concentrator to increase the center field, and also provide self-shielding to minimize the external fringe magnetic field and decrease the normal field in the REBCO coils. To allow the magnetic flux to be concentrated at an optimum state, the iron pole is tapered at an angle of 54.7° [10].

Figure 3 shows a flowchart of the parameter optimization process. On the premise of a 1.5 T center field and no magnetic saturation in the iron yoke, the size of the iron yoke is fixed, as given in table 2. Then, the geometry parameters for the poles and REBCO coils are adjusted simultaneously, until the homogeneity of the center field meets the design requirement. As the center field may no longer be 1.5 T after adjustment, the operating current must be changed, until the center field returns to 1.5 T. Finally, checking the homogeneity again, if the requirement for homogeneity is not met, it is necessary to revise the parameters of the poles and

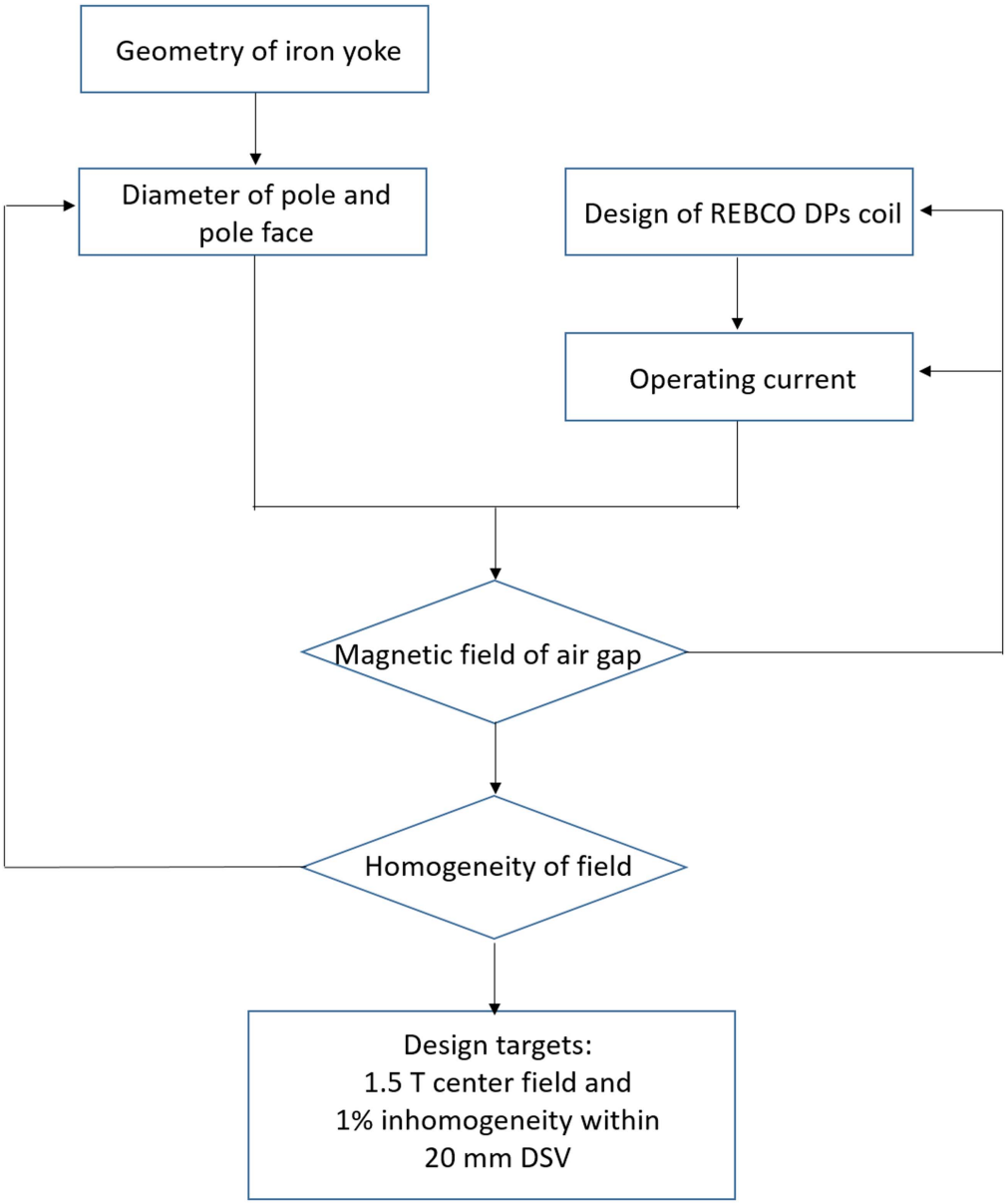

Figure 3. Flowchart of design process. Geometry of iron yoke includes height, width, depth and thickness. Design of REBCO DP coil includes coil geometry design, adjustment of the tape layers for every DP, and the DP amounts for every coil. In the first vision, the height, width, depth and thickness of the yoke are 480, 560, 500 and 75 mm, respectively, the diameter of the pole is 160 mm with a 85 mm pole face, and the REBCO coil is assembled by five single-width (4 mm) DPs (100 layers). After the optimization process, the parameters are adjusted, as given in tables 1 and 2.

REBCO coils, until all the final parameters are optimized, as given in tables 1 and 2.

As the center field is up to 1.5 T, the maximum field in the REBCO coils reaches 0.58 T, with a radial component of 0.44 T and z component of 0.38 T. To estimate the operating current of the studied REBCO coils, angular dependence of I_c (superconducting critical current) for a short sample at 77 K is measured, as shown in figure 4. According to the test results, the I_c of the coils is estimated as 58.2 A. Note that the degradation caused by impregnation and stress is not considered. The maximum operating current is estimated to be within 70% of the coil I_c to ensure safety [11].

2.2. Building of the numerical model

The numerical simulation is based on the finite element method (FEM), and the 3D model is built and computed by COMSOL Multiphysics. To adapt the simulation, the parts of the cryostat and underframe are neglected, while a rectangular air domain is applied. As shown in figure 5, the numerical model is mainly classified into three components, i.e. air domain, iron yoke and poles, and REBCO coils, which are described in detail as follows.

For the air domain, both the relative permeability and relative permittivity are set to be 1. The electrical conductivity is set to be 0 S m^{-1}. To prevent the error of zero division, it

Table 1. Design specifications of the REBCO multi-width DP coil. Thickness of the LN_2 cryostat wall between the pole and REBCO coil is designed as 15 mm, with 1 mm reserved for assembly error. Thus, the inner diameter of the DP coil is set as $125 + 16 \times 2 = 157$ mm. Insulated thickness of the REBCO tape is estimated as 0.3 mm, which gives the DP coil a 211 mm (90 layers) outer diameter. Height of the insulated DP coil is set as $(4 \times 2 + 1) + (4 \times 2 + 1) + (6 \times 2 + 1) = 31$ mm, where 4 mm × 2 is the height of the 4 mm DP and 1 mm is the additional part after insulation. The same applies to the 6 mm DP. Coil I_c estimated by experimental measurement of a short REBCO tape sample.

Parameters	Values
Inner diameter	157 mm
Outer diameter	211 mm
Height	31 mm
Average thickness of every layer	0.3 mm (with insulation)
Turns of every DP	90 × 2
Tape length of every DP	105 m
Number of DPs	2 (4 mm width) + 1 (6 mm width)
Consumption of REBCO tape	210 m (4 mm width) + 105 m (6 mm width) or 367.5 m (4 mm width equivalence)
Estimated coil I_c at 77 K	58.2 A

Table 2. Design specifications of REBCO iron electromagnet. There are three design objectives in this case, i.e. 1.5 T maximum field, at least 30 mm room-temperature gap, 1% spatial inhomogeneity. Instead of 30 mm, a widely used 32 mm gap is adopted in this design. On the premise of three design objectives, the parameters are adjusted as much as possible to reduce the magnet size and consumption of the REBCO tapes.

Parameters	Values
Maximum field in the air gap	1.5 T
Width of air gap	32 mm
Inhomogeneity (20 mm DSV)	0.8%
Maximum operating current	38.7 A
Height of iron yoke	360 mm
Width of iron yoke	480 mm
Depth of iron yoke	160 mm
Thickness of iron yoke	60 mm
Diameter of pole	125 mm
Diameter of pole face	65 mm
Tapered angle of pole	54.7°
Weight of whole magnet	~160 kg
Total consumption of REBCO tape	735 m (4 mm width equivalence)
Capacity of LN_2	~11.7 L

can be set as a small value such as 1 or 10 S m^{-1}, which actually has no influence on the simulation results.

As the iron yoke and poles are ferromagnetic material, the magnetic behavior can be described by the classical magnetization formula:

$$\boldsymbol{B} = \mu_0 \boldsymbol{H}(1 + \chi_m), \quad (1)$$

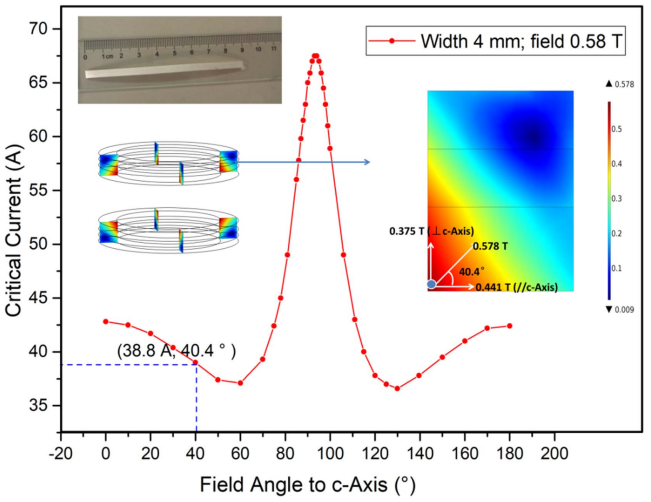

Figure 4. Angular dependence of I_c for a short GdBCO sample at 0.58 T, 77 K. The short sample is cut from long GdBCO tape, which is manufactured by SuNAM Co., Ltd. The width, length and thickness of this sample are 4 mm, 9 cm and 0.16 mm, respectively. The measured I_c is 186 A at 77 K, self-field. In the REBCO coils of the designed magnet, the angle between the maximum magnetic field and *c*-axis is 40.4°. Limited by the test conditions, only 4 mm width tape is available for measuring. Converting it to 6 mm width, the coil I_c is estimated as $38.8^{*}1.5 = 58.2$ A.

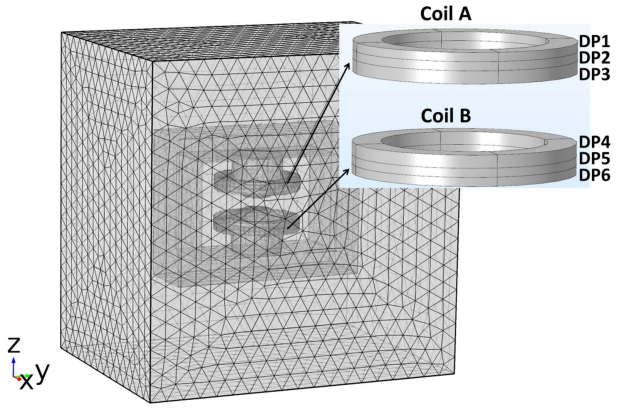

Figure 5. 3D geometry of the FEM model. For convenience, the upper and lower coils are named Coil A and Coil B, respectively. Every coil is assembled by three DPs. DPs are numbered from DP_1 to DP_6.

where $\boldsymbol{B}$ is the magnetic flux density in the yoke and poles. μ_0 is the permeability of the vacuum, which is given the value of $4\pi \times 10^{-7}$ T m^{-1} A^{-1}. Since the magnetic susceptibility χ_m is decided by the material itself and shows nonlinearity to magnetic strength $\boldsymbol{H}$, an interpolation of the nonlinear *B-H* curve of electrical pure iron is adopted as the constitutive relation for the iron yoke and poles, as shown in figure 6. Note that the hysteresis effects are neglected in this case.

For REBCO coils, a homogeneous bulk-like equivalent is constructed to retain the overall electromagnetic behavior [12, 13]. As the material and structure of the iron yoke and poles are given, the simulation results of the magnetic field are only subject to operating current and coil structure, i.e. the number of turns, cross-section area of the tape and the

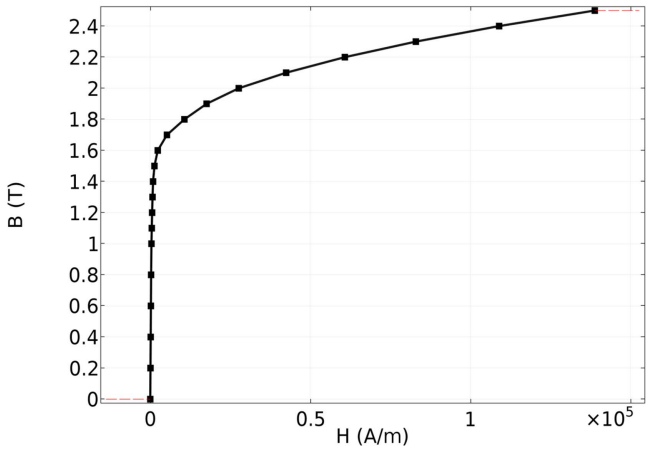

Figure 6. Magnetization curve (*B-H* curve) of electrical pure iron. A nonlinear *B-H* curve that includes saturation effects is used to simulate the magnetic behavior of the iron yoke and poles.

geometry of the coil. To further simplify the simulation, the resistivity of the studied coils is assumed to be isotropic. The resistivity ρ of the REBCO coils is modeled by a power law:

$$\rho(J) = \frac{E_c}{J_c} \cdot \left(\frac{J}{J_c}\right)^{n-1}, \qquad (2)$$

where E_c is the critical current criterion, which is assumed to be 10^{-4} V m^{-1}. J_c is the critical current density of the REBCO coil, and the n value is set as a constant of 20 [14].

3. Results and discussion

3.1. Magnetic field distributions of the whole magnet

The simulation results of the magnetic flux density norm in the whole magnet are shown in figures 7(a) and (b). It is revealed that the iron yoke and poles play a significant role in gathering magnetic flux and increasing the center field. Most of the magnetic flux passes through the iron yoke and air gap to form a magnetic flux circle. As the permeability of air is much lower than ferromagnetic iron poles, magnetic flux naturally diffuses from the iron poles to the air gap. Thus, magnetic flux density in the air gap is dramatically decreased, as shown in figure 8.

Figure 9 shows the relationship between the magnetic field and operating current. The upper curve is the dependence of the magnetic field in the iron pole on operating current. Its slope decreases with the increasing of operating current due to saturation in the pole. The lower curve is the case for the air gap, where the center field is up to 1.5 T as operating current increases to 38.7 A. There are two reasons limiting the center field. The first is the saturation of the pole, which is also adapted for the conventional iron electromagnet. Another is the relatively high B_r component in the REBCO coil. At the 77 K environment, the I_c of the REBCO tape is very sensitive to the magnetic field, and the operating current will be limited by increasing B_r. For the conventional copper-wire one, the operating current will also be limited, due to Joule heat rather than magnetic field.

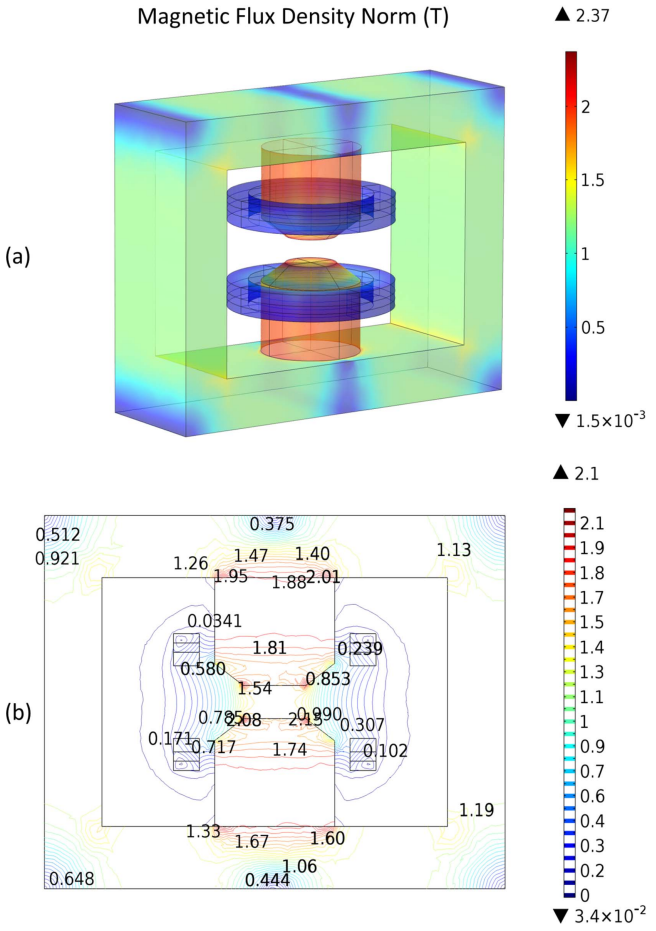

Figure 7. Magnetic flux density norm in the whole magnet. (a) 3D demonstration, (b) 2D contour lines of the center slice (*z-o-y* plane).

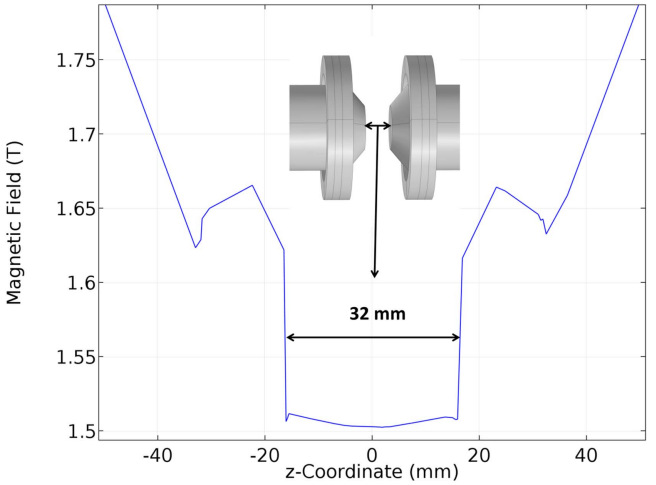

Figure 8. 1D distribution of the magnetic field at the center axis (*z*-axis).

3.2. Homogeneity of magnetic field in the air gap

Based on simulation results, figures 10(a) and (b) reveal that the studied REBCO iron electromagnet provides Φ–20 mm DSV with 0.8% spatial inhomogeneity (peak to peak) of magnetic field in the 32 mm room-temperature gap. Figure 11 demonstrates the homogeneity of the magnetic field in the

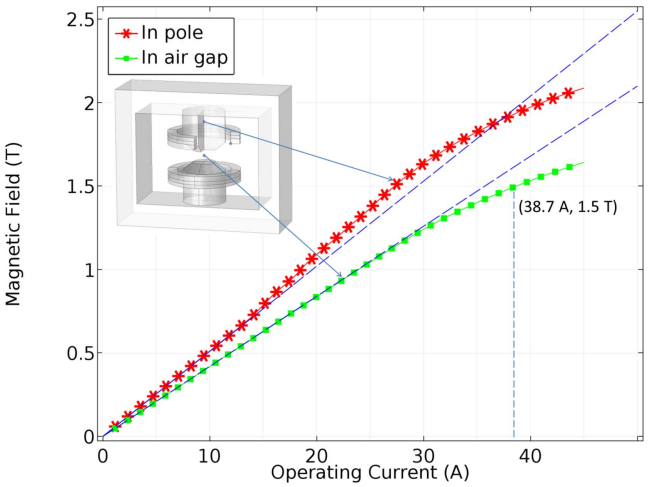

Figure 9. Magnetic field–operating current curve. The center field of the air gap reaches 1.5 T at an operating current of 38.7 A.

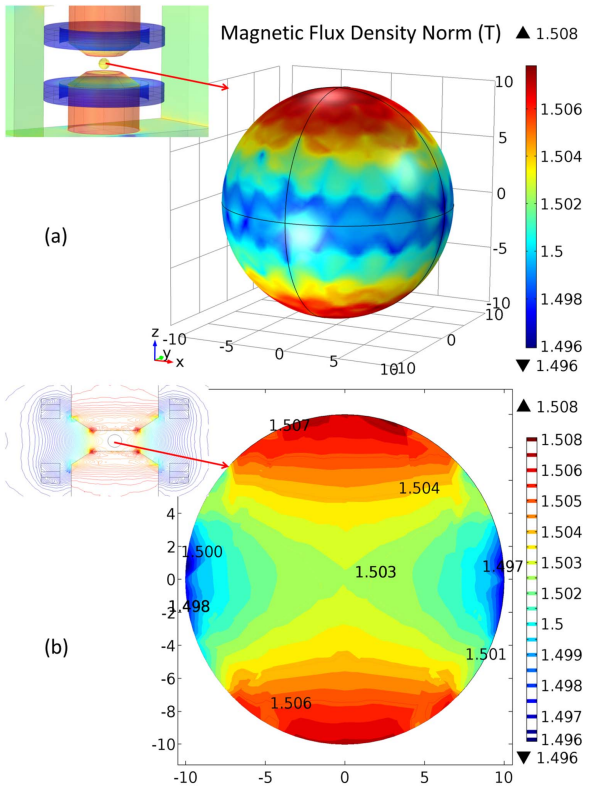

Figure 10. Distribution of magnetic field in the Φ–20 mm DSV of the air gap. (a) 3D depiction, (b) 2D contour lines of the center slice.

radial direction. From $r = 0$ mm to $r = 30$ mm with steps of 5 mm. Cut lines of the magnetic field at different cylindrical radii are given, showing a relatively good magnetic uniformity in the case of $r < 10$ mm, which also implies that the magnetic homogeneity in z direction is better than r direction in the center area. Thus, the inhomogeneity of the magnetic field can be reduced by optimizing the radial distribution. A common method for the conventional iron electromagnet is to enlarge the diameter of the pole and pole face, while this gives rise to other problems, i.e. the size of the whole magnet and the consumption of copper wire or tapes will be

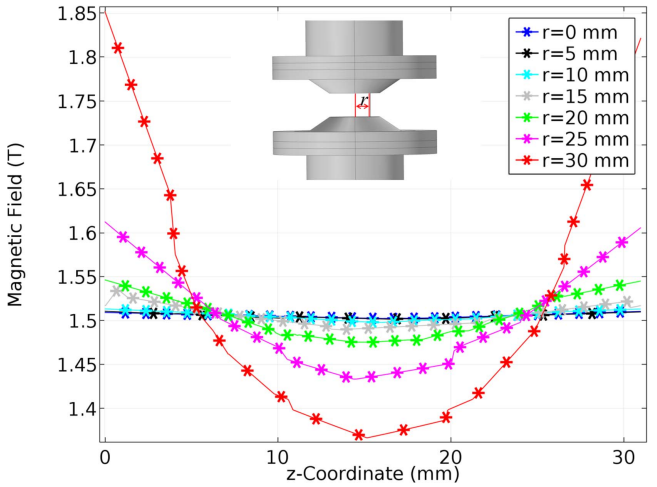

Figure 11. 1D distributions of magnetic field in the air gap at different radii (r).

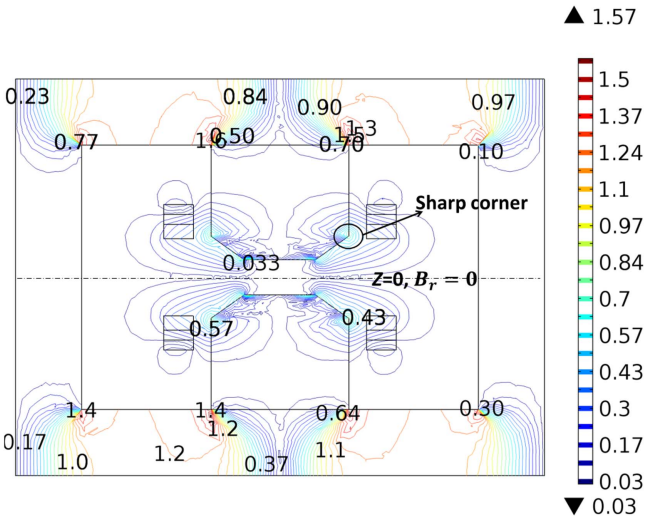

Figure 12. 2D contour lines of B_r in the center splice (z-o-y plane). B_r generated by the two poles is opposite. Thus, in the $z = 0$ plane, B_r is theoretically zero.

increased. In this case, to keep the balance, 0.8% is taken as the final value of field inhomogeneity.

3.3. Radial component of the magnetic field in the REBCO coils

Figure 12 illustrates the general view of B_r in the whole magnet. The contour lines clearly demonstrate a leakage of flux around the sharp corner, leading to a higher strength of B_r in DP_3 and DP_4, which limits the operating current of the whole magnet. Figure 13 demonstrates the distribution of B_r in the REBCO coil. By using a multi-width technique, the 4 mm tape is replaced by wider 6 mm tape at the position of DP_3 and DP_4 to bear a higher B_r as well as a higher operating current. Compared with the previous single-width DP coil, the present multi-width design saves a third of the consumption of REBCO tape.

Figure 14 shows the changes of center field and maximum B_r in the coils corresponding to different d (distance

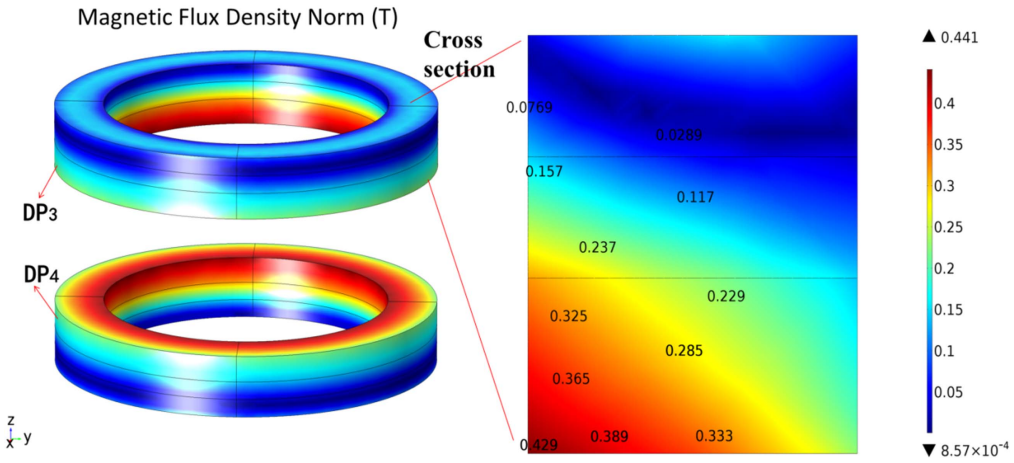

Figure 13. Distribution of B_r in the REBCO coils. The highest B_r appears at the inner corner of DP_3 and DP_4.

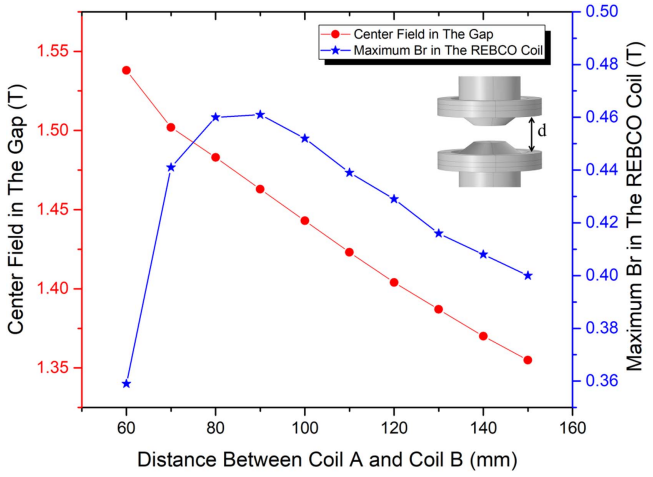

Figure 14. Changes of center field and maximum B_r in the coils corresponding to different d. The distance between Coil A and Coil B changes from 60 to 140 mm with steps of 10 mm. REBCO coils will bear maximum B_r at the distance around $d = 85$ mm.

between Coil A and Coil B). In general, the magnetic flux is easy to diffuse from the sharp corner of the iron pole. This results in relatively high B_r in DP_3 and DP_4. Thus, the B_r in the coils can be reduced by increasing d, i.e. placing two coils far away from the sharp corner. On the other hand, the direction of B_r generated by the two poles is opposite, which implies that the value of B_r on the x-o-y plane ($z = 0$) is theoretically zero. If d is short enough, the maximum B_r in the DP_3 and DP_4 can also be reduced. That means there is a position which generates the highest B_r in the REBCO coils. Nevertheless, increasing d will hamper the center field. Thus, decreasing d should be a better choice. Limited by the structure of the cryostat, the final design of the coil distance is set as $d = 70$ mm.

4. Conclusion

In the present study, the magnetic field distribution of a REBCO iron electromagnet is numerically investigated. To enhance the overall current and reduce the influence of the radial field in the REBCO coil, the multi-width winding technique is applied and the distance between two coils is optimized. Based on the simulation results, the studied magnet can provide variable magnetic fields of 0–1.5 T with a 32 mm room-temperature gap. It is revealed that the spatial inhomogeneity of the field is better than 1% within Φ–20 mm DSV. Compared with the conventional iron electromagnet, the present compact design based on superconducting REBCO tape exhibits smaller volume, lighter weight and lower power consumption, implying better suitability in the case of size limitation.

Acknowledgments

This work was supported by the National Key R&D Program (2016YFF0101701), National Natural Science Foundation of China (51572165) and the Science and Technology Commission of Shanghai Municipality (16521108400, 16DZ0504300 and 14521102800).

ORCID iDs

Shuangrong You https://orcid.org/0000-0002-8078-7119

References

[1] Senatore C, Alessandrini M, Lucarelli A, Tediosi R, Uglietti D and Iwasa Y 2014 Progresses and challenges in the development of high-field solenoidal magnets based on RE123 coated conductors *Supercond. Sci. Technol.* **27** 103001
[2] Weijers H W *et al* 2010 High field magnets with HTS conductors *IEEE Trans. Appl. Supercond.* **20** 576–82
[3] Trociewitz U P, Dalban-Canassy M, Hannion M, Hilton D K, Jaroszynski J, Noyes P, Viouchkov Y, Weijers H W and Larbalestier D C 2011 35.4 T field generated using a layer-wound superconducting coil made of (RE)$Ba_2Cu_3O_{7-x}$ (RE = rare earth) coated conductor *Appl. Phys. Lett.* **99** 202506

[4] Yoon S, Kim J, Cheon K, Lee H, Hahn S and Moon S-H 2016 26 T 35 mm all-$GdBa_2Cu_3O_{7-x}$ multi-width no-insulation superconducting magnet *Supercond. Sci. Technol.* **29** 04LT04
[5] Markiewicz W D *et al* 2012 Design of a superconducting 32 T magnet with REBCO high field coils *IEEE Trans. Appl. Supercond.* **22** 4300704
[6] Juarez E B *et al* 2018 Estimation of losses in the (RE)BCO two-coil insert of the NHMFL 32 T all-superconducting magnet *IEEE Trans. App. Supercond.* **99** 4602005
[7] Yang C K *et al* 2012 Design, fabrication, and performance tests of a HTS superconducting dipole magnet *IEEE Trans. Appl. Supercond.* **22** 4000804
[8] Hahn S, Kim Y, Keun Park D, Kim K, Voccio J P, Bascunan J and Iwasa Y 2013 No-insulation multi-width winding technique for high temperature superconducting magnet *Appl. Phys. Lett.* **103** 173511
[9] Hahn S *et al* 2014 A 78 mm/7 T multi-width no-insulation REBCO magnet: key concept and magnet design *IEEE Trans. Appl. Supercond.* **24** 4602705
[10] Iwasa Y 2009 *Case Studies in Superconducting Magnets-Design and Operational Issues* 2nd edn (Berlin: Springer)
[11] Kim Y G, Hahn S, Kim K L, Yang D G and Lee H G 2015 Design consideration and optimization procedure for a no-insulation multi-width REBCO magnet *Curr. Appl. Phys.* **15** 1134–8
[12] Zermeño V M R and Grilli F 2014 3D modeling and simulation of 2G HTS stacks and coils *Supercond. Sci. Technol.* **27** 044025
[13] Xia J, Bai H, Lu J, Gavrilin A V, Zhou Y and Weijers H W 2015 Electromagnetic modeling of REBCO high field coils by the H-formulation *Supercond. Sci. Technol.* **28** 125004
[14] Nakazono K, Ueda H, Ishiyama A, Noguchi S, Miyazaki H, Tosaka T, Kurusu T, Nomura S, Urayama S and Fukuyama H 2017 Numerical evaluation on irregular field generated by screening current in high-field REBCO coil for whole-body MRI *IEEE Trans. Appl. Supercond.* **27** 4400405